ACADEMIC PRESS

Available online at www.sciencedirect.com

SCIENCE DIRECT®

Analytical Biochemistry 309 (2002) 186–195

ANALYTICAL BIOCHEMISTRY

www.academicpress.com

Physical methods to determine the binding mode of putative ligands for hepatitis C virus NS3 helicase

Ronald W. Sarver,[a,*] Joseph M. Rogers,[a] Brian J. Stockman,[a] Dennis E. Epps,[b] Jack DeZwaan,[a] Melissa S. Harris,[a] and Eric T. Baldwin[a]

[a] *Structural, Analytical and Medicinal Chemistry, 301 Henrietta Street, Kalamazoo, MI 49001, USA*
[b] *Discovery Technologies Pharmacia Inc., 301 Henrietta Street, Kalamazoo, MI 49001, USA*

Received 7 March 2002

Abstract

Several small molecules identified by high-throughput screening (HTS) were evaluated for their ability to bind to a nonstructural protein 3 (NS3) helicase from hepatitis C virus (HCV). Equilibrium dissociation constants (K_d's) of the compounds for this helicase were determined using several techniques including an assay measuring the kinetics of isothermal enzyme denaturation at several concentrations of the test molecule. Effects of two nonhydrolyzable ATP analogs on helicase denaturation were measured as controls using the isothermal denaturation (ITD) assay. Two compounds, 4-(2,4-dimethylphenyl)-2,7,8-trimethyl-4,5-quinolinediamine and 2-phenyl-*N*-(5-piperazin-1-ylpentyl)quinazolin-4-amine, were identified from screening that inhibited the enzyme and had low micromolar dissociation constants for NS3 helicase in the ITD assay. Low micromolar affinity of the quinolinediamine to helicase was also confirmed by nuclear magnetic resonance experiments. Unfortunately, isothermal titration calorimetry (ITC) experiments indicated that a more water-soluble analog bound to the 47/23-mer oligonucleotide helicase substrate with low micromolar affinity as did the substituted quinazolinamine. There was no further interest in these templates as helicase inhibitors due to the nonspecific binding to enzyme and substrate. A combination of physical methods was required to discern the mode of action of compounds identified by HTS and remove undesirable lead templates from further consideration.

Keywords: Hepatitis C virus helicase; Inhibitor; Circular dichroism; Calorimetry; Nuclear magnetic resonance; X-ray crystallography

Disclosure of the complete genomes from many species, including man, and recent advances in proteomics has led to the identification of a large array of enzymes involved in various diseases. To efficiently discover small molecules that may alter the activity of these targeted enzymes, many pharmaceutical companies rely on high-throughput screening (HTS)[1] of large chemical libraries. Each screen can produce, depending upon the size of the chemical library and the robustness of the assay, hundreds of lead compounds. The authenticity of the leads that survive reconfirmation is a concern and must be established using various biochemical and physical secondary assays. Any new methodology that enables this stage of the drug discovery process to proceed more rapidly and with greater accuracy is desirable. Recently, we developed a general method for determining ligand affinities for proteins using a temperature-jump ITD assay that detects changes in the kinetics of protein denaturation upon ligand binding [1]. This work showed that the rate constants measured for the denaturation of thymidylate kinase and stromelysin were independent of the detection method. The detection methods utilized included fluorescence, circular dichroism (CD), and UV hyperchromicity spectroscopy. The ITD method with fluorescence detection is also applicable for HTS and particularly attractive for proteins with yet undetermined function.

* Corresponding author. Fax: 1-616-833-1822.
E-mail address: ronald.w.sarver@am.pnu.com (R.W. Sarver).

[1] *Abbreviations used:* CD, circular dichroism; CHAPS, 3-[(3-cholamidopropyl)dimethylammonio]-1-propanesulfonate; DAPI, 4,6-diamidino-2-phenylindole DSC, differential scanning calorimetry; ITC, isothermal titration calorimetry; ITD, isothermal denaturation; HCV, hepatitis C virus; HTS, high-throughput screening; MOPS, 3-[*N*-morpholino]propanesulfonic acid; NMR, nuclear magnetic resonance; NS3, nonstructural protein 3.

0003-2697/02/$ - see front matter © 2002 Elsevier Science (USA). All rights reserved.
PII: S0003-2697(02)00301-9

Several lead compounds discovered by screening a helicase from hepatitis C virus (HCV) were evaluated using various biophysical techniques including ITD. Finding an effective treatment for HCV is of great interest since the virus infects millions of people worldwide and, in a significant number of cases, leads to cirrhosis and hepatocellular carcinoma [2,3]. Since the virus has several different subtypes, finding an effective vaccine has proven elusive and currently approved drug therapies are effective in less than half of patients with chronic HCV [2,3].

The genome from HCV encodes a nonstructural protein 3 (NS3) helicase. NS3 helicase is a nucleoside triphosphate (NTP)-dependent enzyme that unwinds duplexed RNA and DNA substrates involved in viral replication. This helicase is a three-domain protein containing an NTP-binding site on domain 1 and an oligonucleotide-binding site located at the hinge region between domains 1 and 2 [4–6]. Although the mechanism of action is unclear, it is known that duplex unwinding is coupled to ATP hydrolysis and requires a divalent metal ion cofactor [7]. Small molecules that bind to either the ATP or the oligonucleotide-binding site may interfere with enzyme catalysis and inhibit viral replication. The enzyme therefore provides an attractive target for drug design to treat hepatitis C and has received much attention recently.

In the work we present here, the kinetics of helicase ITD were examined in the presence of two nonhydrolyzable ATP analogs, an oligonucleotide substrate, and several putative small molecule inhibitors of the enzyme. Lead compounds were initially chosen since they inhibited enzymatic activity but additional experiments were required to determine the affinity, mode, and specificity of binding interactions. For some compounds, NMR spectroscopy, isothermal titration calorimetry, and X-ray crystallography were also used to support the optical methods of denaturation monitoring. The use of these techniques in concert with each other provided complementary data enabling us to better determine the mode of inhibition for the putative ligands.

Materials and methods

NS3 helicase and substrate

Active truncated HCV-1 NS3 helicase (MW = ~50 kDa) from yeast *Saccharomyces cerevisiae* was provided by Chiron Co. (Emeryville, CA) in 50 mM Tris, pH 8.0, 0.5 M NaCl, 10% glycerol, 0.1% octylglucopyranoside, 5 mM BME [8]. Concentration of the stock NS3 helicase solution was 5 mg/ml as determined by quantitative amino acid analysis. Concentrations of helicase dilutions were checked using an absorptivity at 280 nm of 88.5 $L\,mM^{-1}\,cm^{-1}$. The amino acid sequence of the HCV-1 genotype 1a construct used in this work consisted of 465 amino acids from the NS3 protein numbered 1193 to 1657 as previously described [8].

The 47/23-mer oligonucleotide substrate was purchased from Oligo's Etc. (Wilsonville, OR) and comprised the following sequence: 3′-TGAACTAACTACC AGTATCGACAAATCATGGCGGTGGGAGTCTTG AT and 5′-TAGTACCGCC ACCCTCAGAACTG.

Compounds identified from high-throughput screening were obtained from the research compound collection at Pharmacia. Structures for some of the compounds tested are shown in Fig. 1. The nonhydrolyzable ATP analog, β, γ-difluoromethyleneadenosine-5′-triphosphate (AMP-PCF_2P) (**1**) was obtained from C. Bystrom. The preparation of (**1**) has been described [9]. A compound identified from screening, 4-(2,4-dimethylphenyl)-2,7,8-trimethyl-4,5-quinolinediamine (**2**) was obtained from Brandon/SPECS Inc. (The Hague, the Netherlands). DAPI (4′,6-diamidino-2-phenylindole dihydrochloride hydrate), AMP-PNP, and Chaps were purchased from Sigma Chemical Co. as were all buffer components. Water used in all buffer preparations was purified with a Millipore Milli-Q purification system.

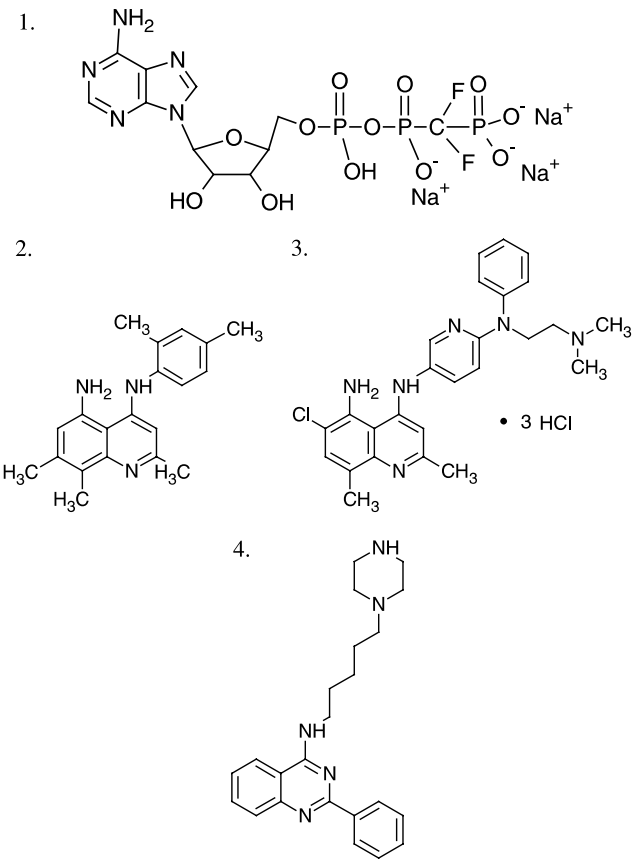

Fig. 1. Structures and chemical names of compounds examined: (1) β, γ-difluoromethyleneadenosine 5′-triphosphate (AMP-PCF_2P), (2) 4-(2, 4-dimethylphenyl)-2,7,8-trimethyl-4,5-quinolinediamine, (3) 6-chloro-*N*-4-{6-[[2-(dimethylamino)ethyl](phenyl)amino]pyridin-3-yl}-2,8-dimethylquinoline-4,5-diamine·HCl, and (4) 2-phenyl-*N*-(5-piperazin-1-yl-pentyl)quinazolin-4-amine.

Differential scanning calorimetry

DSC scans were obtained using a VP-DSC differential scanning calorimeter from Microcal, Inc. (Northampton, MA) [10]. The DSC parameters were set to obtain 10 identical scans from 25 to 90 °C with a prescan thermostat of 15 min at 25 °C, a postscan thermostat of 5 min at 80 °C, 16-s filtering period, a scan rate of 1 °C/min, and collection in passive feedback mode. The 0.51-ml sample and reference cells of the calorimeter were carefully filled with 10 mM Hepes, 1 mM $MgCl_2$, pH 7.2, and the scan set was started. After collection of three baseline scans to establish a consistent thermal history, 0.5 ml of 14.6 μM HCV helicase in 10 mM Hepes, 1 mM $MgCl_2$, pH 7.2, was injected into the sample cell after the calorimeter reached 25 °C and the scans were continued. All solutions were degassed for 5 min prior to loading the calorimeter. Baseline DSC scans collected with dialysate buffer in the sample cell were subtracted from the protein DSC scans and the resulting data normalized by protein concentration. The DSC *Y*-axis was calibrated using known electrical heat pulses. Temperature calibration was performed using *n*-octadecane and *n*-hexatriacontane standards that melt at 28.2 and 75.9 °C, respectively. The DSC standards were provided by Microcal Inc. in sealed vessels that fit directly into the calorimeter.

Circular dichroism spectroscopy

Circular dichroism spectra of HCV helicase were acquired using a Jasco (Easton, MD) J-715 spectrophotometer and thermostated cylindrical quartz cells with a Haake D8 circulating water bath controlled to within 0.1 °C. A far-UV CD spectrum was collected at 23 °C using 2.9 μM helicase in 10 mM Hepes, pH 7.2, 1 mM $MgCl_2$, and 0.1% Chaps at a pathlength of 0.1 cm. Solution volume was 200 μl. Far-UV CD spectra were collected from 178–260 nm with a response of 0.25 s, scan speed of 100 nm/min, resolution and bandwidth of 1.0 nm, and 5 accumulations. The CD response was calibrated with ammonium-D-camphor-10-sulfonate.

Background-subtracted CD spectra were imported into Grams/32 for conformational analysis using principal component regression analysis [11,12]. Helicase secondary structure was determined using a basis set of CD spectra for 16 different proteins of known secondary structure obtained from Hennessey and Johnson [13] and Compton and Johnson [14]. The method is similar to that described in the previous references but was adapted to run on a commercially supplied software package (PLSplus/IQ version 3.02) obtained from Galactic Industries (Salem, NH). The basis set comprise a mean centered CD data in units of $\Delta\varepsilon$ (L/mol cm) from 195 to 260 nm at 1 nm resolution along with the X-ray crystallographic secondary structure percentages for α-helix, parallel and antiparallel β-sheet, β-turn, and other or random structure [13]. Basis set data were mean-centered by subtracting the average spectrum from each of the library entries. Five factors provided the optimum agreement between experimental and known secondary structure percentages. To estimate the conformational percentages of helicase solutions, the experimentally obtained CD spectra were converted to units of $\Delta\varepsilon$ (L/mol cm) and analyzed using the five most significant principal components.

Helicase isothermal denaturation kinetics followed by UV detection

Isothermal denaturation kinetics detected by the change in UV absorbance were conducted using a Perkin–Elmer Lambda 40 UV–Vis dual-beam spectrophotometer. Capped 1.0 cm pathlength quartz cuvettes filled with 1.5 ml of assay buffer (10 mM Hepes, 5 mM $MgCl_2$, 0.1% Chaps, pH 7.2) were placed in the sample and reference beams. The cuvette in the sample beam was held at 46 °C, a temperature near the midpoint of the protein's thermal transition as determined by DSC. Cuvette temperature was maintained using a Neslab Exacal EX200 circulating water bath controlled to within 0.1 °C as monitored by a VWR digital thermometer. Stable baseline absorbance readings were obtained after 5 min equilibration at 46 °C. Control experiments were conducted by adding 2 μl of stock NS3 helicase solution to the sample cell containing 1.5 ml of assay buffer. The final NS3 helicase concentration was 133 nM except for initial AMP-PCF_2P experiments in which the concentration was 0.6 μM. The absorbance of this solution at 280 nm was collected every 1 s for up to 30 min with a bandwidth of 2 nm and response of 0.5 s. For affinity measurements, the test compound, at a starting concentration of 1 μM, was added to buffer (held at 46 °C) in the sample cuvette. Compound stability at 46 °C was monitored prior to enzyme addition by following the absorbance at 280 nm for 5–10 min to ensure the compound absorbance did not change greater than 5 milliabsorbance units. The compound absorbance was then zeroed, helicase added, and the denaturation kinetics monitored in the presence of compound. Additional experiments were performed at several concentrations of compound usually up to about 100 μM. All solutions were degassed for 5 min prior to data collection. Cuvettes were thoroughly cleaned with nitric acid plus 10% methanol and rinsed with distilled water and ethanol between experiments.

Kinetics of isothermal denaturation followed by fluorescence detection

The kinetics of isothermal denaturation were also monitored continuously with stirring using an ISS PC-1 spectrofluorometer at $T = 46$ °C as described previously

[1]. A brief description of the method follows. A fluorescent dye, in this case SYPRO red, that binds to hydrophobic regions of protein exposed upon denaturation is added to buffer and equilibrated near the unfolding point of HCV helicase, 46 °C. SYPRO red has a low quantum yield in an aqueous environment that increases several-fold when bound to the exposed hydrophobic regions of the enzyme as it unfolds. Protein is then injected into a solution of dye and buffer with or without putative ligand and the change in fluorescence recorded versus time. Protein concentration was 0.25 μM and dye was diluted 1:20,000. SYPRO red was purchased from Molecular Probes, Inc. (Eugene, OR). The fluorescence data were best analyzed by a model of two parallel first-order reactions indicating the unfolding reaction proceeded in at least two steps.

Kinetic analysis of NS3 helicase isothermal denaturation data

Denaturation of NS3 helicase followed by the change in absorbance at 280 nm was consistent with a composite reaction of the type

$$A \overset{k_1}{\rightarrow} B \overset{k_2}{\rightarrow} C.$$

Preliminary data analysis of NS3 helicase denaturation at 46 °C indicated the rate constants k_1 and k_2 were nearly equivalent. In this case, we have previously shown [1] that the following equation can be used to fit the experimental data:

$$Y = Y_A \cdot e^{-k \cdot t} + Y_B \cdot k \cdot t \cdot e^{-k \cdot t} + Y_C \cdot \left[1 - (k \cdot t + 1)e^{-k \cdot t}\right], \quad (1)$$

where Y is the experimentally measured signal, Y_A, Y_B, and Y_C are the signals for component A, B, and C, respectively, k is the overall rate constant, and t is time. Apparent dissociation binding constants, K_d's, were then obtained by nonlinear least-squares analysis of the rate constant versus ligand concentration data using the equation for a simple Langmuir-binding isotherm.

The ligand concentration for the control experiment was set at a nominal concentration of 10 nM to plot the control data on the log scale. For quick K_d estimations, absorbance values at 280 nm at a set time point (18 min) after initiating denaturation were also fit using a simple Langmuir-binding isotherm.

NMR spectroscopy

The stock helicase solution was exchanged into a solution containing 50 mM [^{2}H]imidazole, 50 mM NaCl, and 5 mM [^{2}H]DTT at pH 7.3 with 10 washes through a 3 K molecular weight cutoff Nanosep tube. To make the NMR samples, 200 μl of this helicase protein solution was added to 300 μl of ^2H_2O, followed by 7 μl of 3.6 mM quinolinediamine (**2**) dissolved in [^{2}H]DMSO solution. For the control samples, 200 μl of the helicase exchange buffer was used in place of the helicase protein solution. The final samples were approximately 50 μM ligand and, if present, 40 μM helicase. Addition of equimolar poly(dU)$_{15}$ was accomplished by adding a small amount of concentrated aqueous stock solution to the NMR samples.

A stock solution of *D. vulgaris* flavodoxin containing 1 mM protein in 100 mM phosphate buffer at pH 6.5 was used to prepare the flavodoxin samples. To make the NMR samples, 20 μl of this flavodoxin protein solution was combined with 50 μl of ^2H_2O, 430 μl of phosphate buffer (100 mM at pH 6.5), and then 7 μl of 3.6 mM quinolinediamine (**2**) dissolved in [^{2}H]DMSO solution. For the control samples, an additional 20 μl of the phosphate buffer was used in place of the flavodoxin protein solution. The final samples were approximately 50 μM ligand and, if present, 40 μM flavodoxin.

All NMR spectra were collected on a Bruker DRX-500 spectrometer. All experiments were collected at 27 °C using a 5-mm 3-axis gradient, triple-resonance probe. One-dimensional relaxation-edited ^{1}H NMR spectra [15] were collected on each sample. The spin-lock time used was 350 ms. Presaturation was used to suppress the water resonance.

Isothermal titration calorimetry

Isothermal titration calorimetry experiments were performed using an OMEGA titrating microcalorimeter from Microcal, Inc. (Northampton, MA). Data collection, analysis, and plotting were performed using a Windows-based software package (Origin 5.0) supplied by the instrument vendor. The titrating microcalorimeter consisted of a sample and reference cell held in an adiabatic enclosure. The calorimeter was calibrated by comparing the measured areas of applied heat pulses to known values. Known and experimentally measured values agreed to within 2%.

Stock 47/23-mer oligonucleotide (MW = 21.6 kDa) solution was dialyzed against 50 mM Mops, pH 6.5, 2 mM Chaps, 0.4 mM ATP, 0.4 mM $MgCl_2$ using a Pierce Slide-A-Lyzer mini dialysis unit with a 7000 molecular weight cutoff membrane. To minimize heat of dilution effects resulting from differences in buffer composition between test compound and 47/23-mer substrate, the compound was dissolved in dialysate buffer. The concentration of oligonucleotide was determined using an OD of 1.5 at 260 nm for a 2.2 μM solution of duplexed oligonucleotide. Test compound and substrate solutions were degassed prior to analysis. The reference cell was filled with dialysate buffer. Buffered 47/23-mer substrate solution (10 μM) was placed

in the 1.37 ml-sample cell and the test compound (2 mM) held in a 250-μl syringe. Typically, 30 injections (8 μl each) of ligand were made by a computer-controlled stepper motor into the sample cell filled with 47/23-mer substrate solution held at 37 °C. The syringe stir rate was 400 rpm. The heat adsorbed or released with each injection was measured by a thermoelectric device connected to a Microcal nanovolt preamplifier. Titration isotherms for the binding interactions were composed of the differential heat flow for each injection. Heats of dilution obtained by injecting ligand into dialysate buffer were minor but were subtracted prior to fitting the data. Isotherms fit well to a two sets of independent sites model (equation provided in reference [16]) using an iterative nonlinear least-squares algorithm included with the instrument.

All parameters were floated during the iterations until a minimum χ^2 was obtained between experimental and fit data. Deconvolution of the isotherms by this method provided the binding constant, K, change in enthalpy, ΔH, and stoichiometry, N, of binding for each interaction. The change in free energy (ΔG) and change in entropy (ΔS) were determined using the Gibbs' free energy equation.

X-ray crystallography

Tetragonal crystals of helicase were prepared without compounds. The crystals were soaked with 5 mM compound overnight, then frozen in liquid nitrogen, and stored for later data collection at APS Argonne National Lab. Data were collected on 17-ID using the MAR CCD. Details of the crystallization and structure determinations have previously been described [17].

Results

Circular dichroism spectra of HCV helicase

Fig. 2 shows the far-UV CD spectra of native and heat-denatured HCV helicase in 10 mM Hepes, 1 mM $MgCl_2$, pH 7.2. Principal component analysis of the spectrum from native HCV helicase indicated the following secondary structure percentages; 30% α-helix, 4% parallel β-sheet, 11% antiparallel β-sheet, 15% β-turn, and 39% disordered coil. The error in the conformational analysis of spectra in the calibration matrix was ±5%. The α-helix percentage was consistent with analysis of the NS3 helicase structure determined by X-ray crystallography indicating that 176 of 465 residues (38%) were involved in an α-helix and 92 of 465 residues (20%) were in a β-sheet.

Fig. 3 shows the DSC scan of NS3 helicase with an endothermic transition centered at 46 °C due to enzyme unfolding. Above 50 °C, the enzyme precipitated as indicated by the exotherm detected in the DSC scan. Unfolding of the enzyme at 46 °C was confirmed by the CD ellipticity change at 222 nm, suggesting a conformational alteration that resulted in a loss of helical structure. The CD spectrum of heat-denatured helicase is shown only to 217 nm in Fig. 2. At lower wavelengths, significant noise was detected due to light scattering from aggregate formation.

Effect of nonhydrolyzable ATP analogs on the isothermal denaturation kinetics of HCV helicase

Protein denaturation can be followed readily by changes in absorbance near 280 nm that occur when chromophores buried in hydrophobic environments are

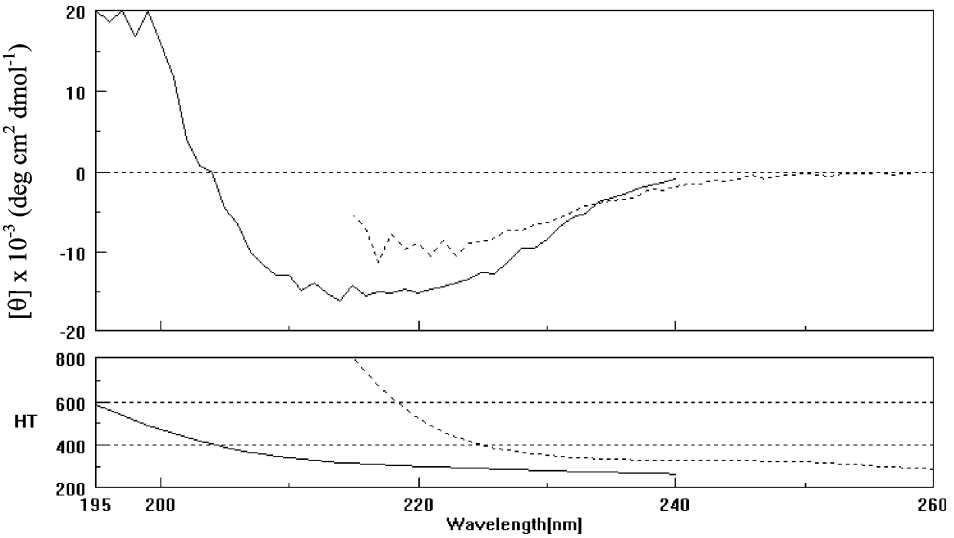

Fig. 2. Far-UV CD spectra of 2.9 μM HCV NS3 helicase (solid line) and 2.9 μM helicase denatured at 46 °C (short dashed). Each solution was prepared in 10 mM Hepes, 1 mM $MgCl_2$, pH 7.2. Bottom panel is a plot of the high-voltage reading on the photomultiplier tube for each spectrum.

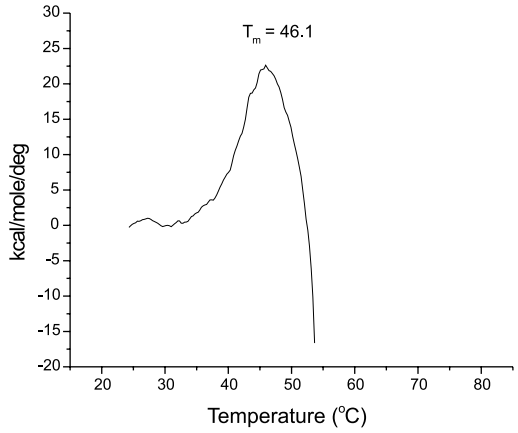

Fig. 3. DSC of 14.6 μM HCV helicase in 10 mM Hepes, 1 mM MgCl2, pH 7.2.

exposed to solvent as the protein denatures. Fig. 4 shows the time-dependent change in absorbance at 280 nm for HCV helicase as it isothermally denatures in buffer at 46 °C. NS3 helicase binds ATP at a site on domain I and is required for enzyme activity. Thus it was expected that the nonhydrolyzable ATP analogs AMP-PCF_2P and AMP-PNP would bind to helicase in a similar fashion. Figs. 4A and B show the effects AMP-PCF_2P had on the denaturation rate of NS3 helicase as measured by UV absorbance and fluorescence spectroscopy, respectively. AMP-PCF_2P destabilized the enzyme in a dose-dependent manner using both detection methods as evidenced by an increased rate of change in SYPRO red fluorescence and helicase hyperchromicity with increasing compound concentration. Table 1 lists rate constants for NS3 helicase denaturation at 46 °C obtained from nonlinear least-squares fitting of the experimental data shown in Fig. 4A using Eq. (1). Increasing concentrations of AMP-PCF_2P accelerated the denaturation of helicase. At 46 °C with 266 μM AMP-PCF_2P added, enzyme denaturation was too rapid to allow saturating levels of the compound to be added. Therefore, we could not determine an equilibrium -binding constant but were able to confirm that alteration of the enzyme denaturation rate occurred in the presence of bound AMP-PCF_2P.

Fig. 5A shows the dose response alteration of helicase denaturation rate with AMP-PNP. Converse to AMP-PCF_2P, AMP-PNP produced a stabilizing effect with a nearly saturated binding isotherm at 400 μM. Fig. 5B shows the dose response for AMP-PNP's stabilizing effect on the denaturation rate of helicase using the absorbance values at 280 nm after 400 s of denaturation. The solid line in Fig. 5B resulted from nonlinear least-squares fitting of the data using the equation for a Langmuir-binding isotherm. The data were well fit using this equation and indicated an apparent K_d of 260 μM.

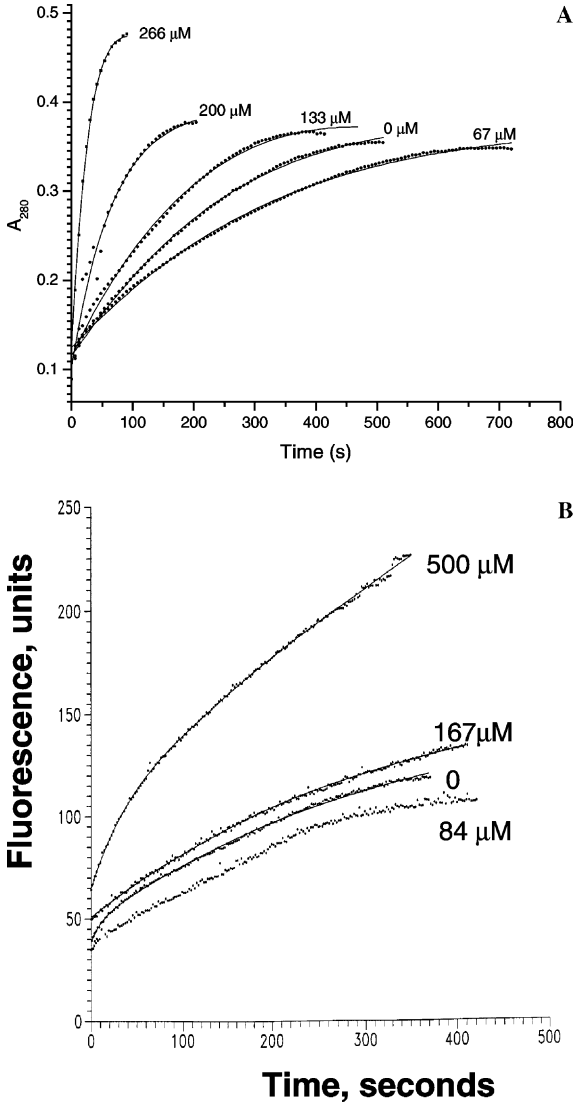

Fig. 4. (A) Effect of AMP-PCF_2P on the isothermal denaturation rate of 0.6 μM HCV helicase followed by $\Delta A_{280\,nm}$ vs time at 46 °C in 10 mM Hepes, 5 mM $MgCl_2$, pH 7.2. Curves are listed with the concentrations of AMP-PCF_2P that were added to buffer prior to enzyme addition. The solid lines are the results from nonlinear least-squares curve fitting the experimental data using Eq. (1) as described under Materials and methods. (B) Effect of AMP-PCF_2P on the isothermal denaturation rate of 0.6 μM HCV helicase followed by the change in fluorescence of SYPRO-red vs time at 46C in 10 mM Hepes, 5 mM $MgCl_2$, pH 7.2. Curves are listed with the concentrations of AMP-PCF_2P that were added to buffer prior to enzyme addition.

Table 1
Effect of a nonhydrolyzable ATP analog on the rate constants for isothermal denaturation of NS3 helicase

[AMP-PCF_2P] (μM)	k (min^{-1})
0	0.27
67	0.24
133	0.39
200	0.90
266	1.4

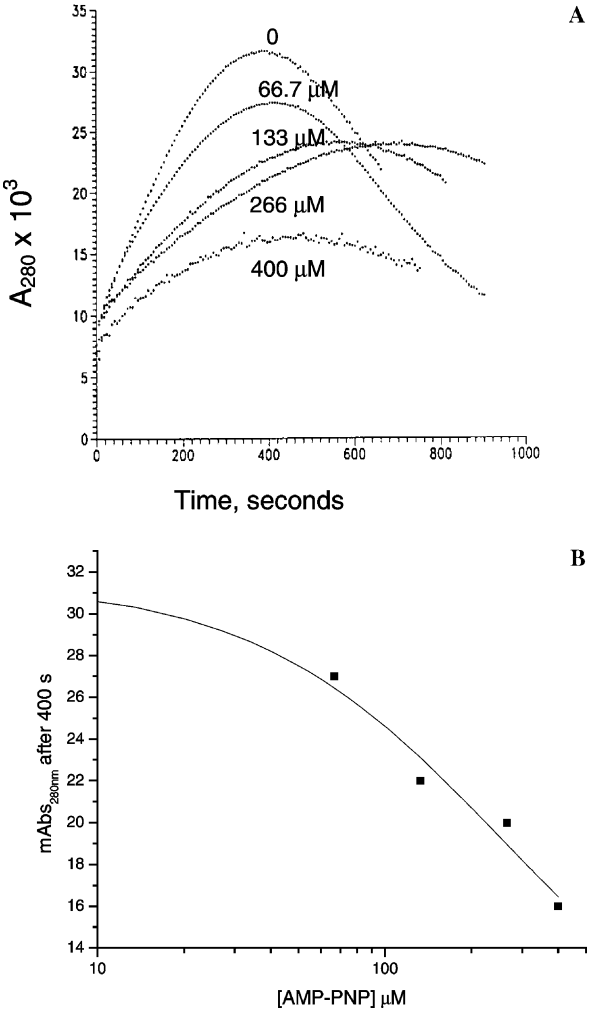

Fig. 5. (A) Effect of AMP-PNP on the isothermal denaturation rate of 0.6 μM HCV helicase followed by $\Delta A_{280\,nm}$ vs time at 46 °C in 10 mM Hepes, 5 mM $MgCl_2$, pH 7.2. Curves are listed with the concentrations of AMP-PNP that were added to buffer prior to enzyme addition. (B) Dose-dependency for the effect of AMP-PNP on the isothermal denaturation of HCV NS3 helicase by UV hyperchromicity. The solid line represents the theoretical fit to the experimental data points (squares) using a Langmuir-binding isotherm as discussed under Materials and methods.

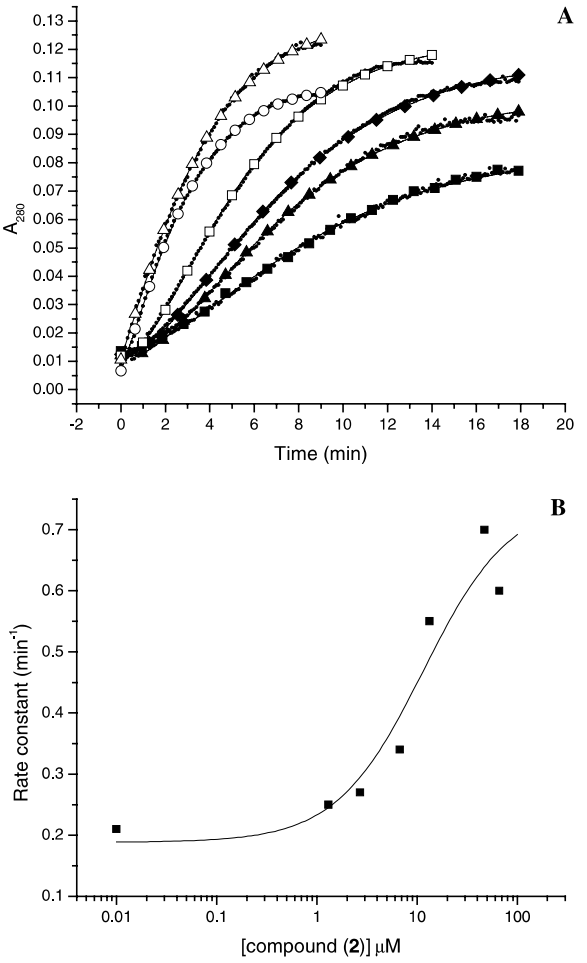

Fig. 6. (A) Effect of increasing concentration of 4-(2,4-dimethylphenyl)-2,7,8-trimethyl-4,5-quinolinediamine (0 μM, solid squares; 1.3 μM, solid triangles; 2.7 μM, solid diamonds; 6.7 μM, open squares; 13 μM, open circles; and 47 μM, open triangles) on isothermal denaturation rate of HCV Helicase in 10 mM Hepes, 5 mM $MgCl_2$, pH 7.2, 0.1% Chaps. The solid lines are the results from nonlinear least-squares curve fitting the experimental data using Eq. (1) as described under Materials and methods. (B) Dose-dependency for the effect of 4-(2,4-dimethylphenyl)-2,7,8-trimethyl-4,5-quinolinediamine on the isothermal denaturation of HCV NS3 helicase by UV hyperchromicity. The solid line represents the theoretical fit to the experimental data points (squares) using a Langmuir-binding isotherm as discussed under Materials and methods.

Alteration of helicase denaturation kinetics by 4-(2,4-dimethylphenyl)-2,7,8-trimethyl-4,5-quinolinediamine

Several lead molecules identified from high-throughput screening of the Pharmacia collection were examined in the isothermal denaturation assay with UV detection. Shown in Fig. 6A are the raw isothermal denaturation data of helicase with increasing concentration of 4-(2,4-dimethylphenyl)-2,7,8-trimethyl-4,5-quinolinediamine (**2**), subsequently referred to as phenyl quinolinediamine. The denaturation rate of the control was reproducible and increasing concentrations of the phenyl quinolinediamine produced a dose-dependent increase in the rate constant for enzyme denaturation. The solid lines shown in Fig. 6A result from nonlinear least-squares fitting of the data using Eq. (1). The data were consistent with the experimental model as evidenced by the agreement of the experimental data points and the theoretical curves. Fig. 6B shows a plot of the isothermal denaturation rate constants as a function of phenyl quinolinediamine concentration. The data were fit using the equation for a simple Langmuir-binding isotherm resulting in an apparent K_d for the interaction of 17 μM. The effect was saturable with a slope slightly steeper than a two log change in phenyl quinolinediamine concentration.

NMR spectroscopy of 4-(2,4-dimethylphenyl)-2,7,8-trimethyl-4,5-quinolinediamine and HCV helicase

One-dimensional relaxation-edited ^{1}H NMR spectroscopy was used to monitor the interaction of the phenyl quinolinediamine (**2**) with HCV helicase. With this technique, a reduction in resonance intensity is observed for a given compound if it interacts with the receptor protein. The spectra obtained for the phenyl quinolinediamine in the absence and presence of helicase are shown in Fig. 7. In control relaxation-edited ^{1}H NMR spectra collected in the absence of protein, resonances from phenyl quinolinediamine were observable (Fig. 7A). In the relaxation-edited ^{1}H NMR experiments in the presence of helicase, resonances from the protein and ligand disappear (Fig. 7B). For the phenyl quinolinediamine, this is evident for all of its resonances in the region shown (2.14–2.41, 6.09, 6.99, 7.18, and 7.26 ppm). Buffer resonances, which are still observable in all spectra with the spin-lock time used, indicate that the observed effect is specific for the phenyl quinolinediamine, and not a general effect on small molecules present in the samples. The phenyl quinolinediamine appears to bind tightly to helicase from the NMR data. Since fast exchange between free and bound ligand is not observed, it is difficult to derive a K_d value from this analysis. Qualitatively, the binding must be at least low micromolar. Addition of equimolar poly$(dU)_{15}$ to the helicase/phenyl quinolinediamine solution resulted in no detectable changes in the helicase/phenyl quinolinediamine interactions. However, noticeable sample precipitation occurred making the spectra difficult to interpret.

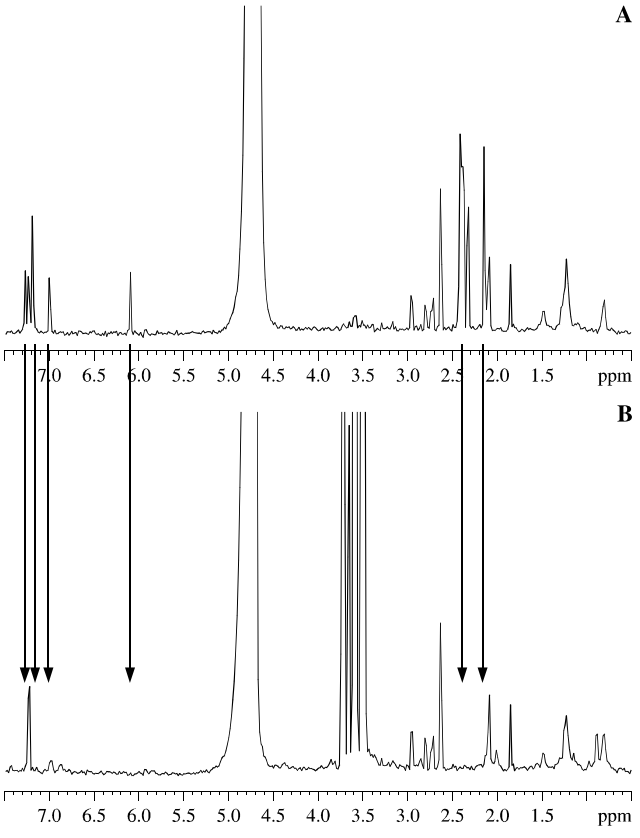

Fig. 7. One-dimensional relaxation-edited ^{1}H NMR spectra of solutions containing 4-(2,4-dimethylphenyl)-2,7,8-trimethyl-4,5-quinolinediamine and (A) HCV helicase buffer or (B) HCV helicase protein. Arrows identify resonances from 4-(2,4-dimethylphenyl)-2,7,8-trimethyl-4,5-quinolinediamine that experience a significant reduction in intensity in the presence of protein. Note that the sharp buffer resonances at 1.85, 2.10, and 2.6–3.0 ppm are not affected. The strong resonances between 3.5 and 3.8 ppm in (B) arise from residual glycerol that is present in the protein solution but not in the buffer solution.

Similar relaxation-edited data sets were collected for the phenyl quinolinediamine against a control protein: flavodoxin. For this compound with the control protein, the same result was observed as for helicase. No ligand signals were observed when a relaxation filter was applied. Data sets were also collected for the compound by itself with no added protein to verify that these free-ligand signals were still observed when a relaxation filter was applied. Applying the same interpretation as for the helicase data, the phenyl quinolinediamine binds to flavodoxin.

Substrate 47/23-mer DNA binding of a substituted quinolinediamine hydrochloride salt determined by isothermal titrating calorimetry

Although poor aqueous solubility of phenyl quinolinediamine (**2**) precluded isothermal titrating calorimetry analysis to check for binding of the molecule to HCV helicase substrate, a more water-soluble analog, 6-chloro-*N*-4{6[[2(dimethylamino)ethyl](phenyl)amino] pyridin-3-yl}-2,8-dimethylquinoline-4,5-diamine. HCl (**3**) was examined, subsequently the compound is referred to as a pyridinyl quinolinediamine. The top panel of Fig. 8 shows the heat flow per 8-μl injection of the pyridinyl quinolinediamine into 47/23-mer DNA substrate and the heat of dilution of the ligand into buffer. The heat of dilution of ligand into buffer was small and endothermic. The bottom panel of Fig. 8 shows the integrated heats for each injection and the best fit line from the two independent sites model used. The agreement between the model and the data was very good and indicated one site had an affinity of 3.0 μM while the other was about 10-fold less tightly bound at 32.3 μM. The stoichiometry of the highest affinity interaction indicated one ligand molecule bound per every other base pair with a ΔH of −2.9 kcal/M, ΔG of −7.8 kcal/M, $T\Delta S$ of 4.9 kcal/M. This entropy term was favorable and indicated a large portion of the interaction derived energy from the change in entropy. The stoichiometry for the lower affinity site also indicated one ligand bound per every other base pair. Although the lower affinity interaction was more exothermic with a ΔH of

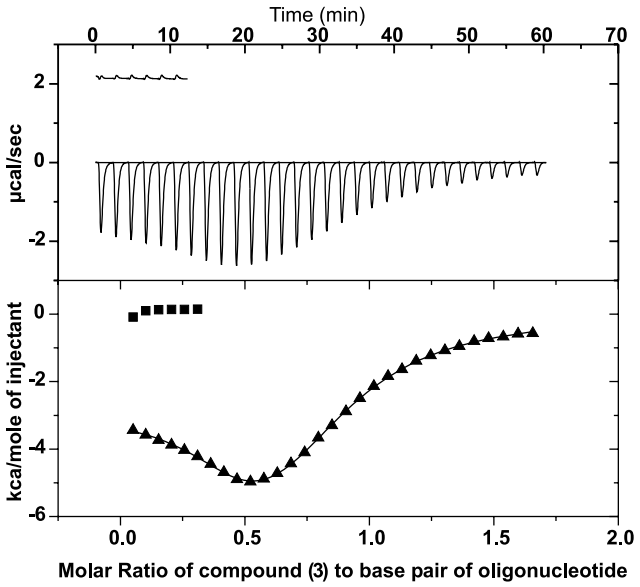

Fig. 8. Top panel, isothermal titrating calorimetry results for 30 injections, 8 µl each, of 2 mM compound (**3**) into 10 µM 47/23-mer DNA oligonucleotide at 37 °C. Also shown is the heat of dilution for 6 injections, 8 µl each, of compound (**3**) into the same buffer, 50 mM Mops, pH 6.5, 2 mM Chaps, 0.4 mM ATP, 0.4 mM Mg. Bottom panel, integrated enthalpy change for each injection of compound into oligonucleotide (triangles). The solid line is the theoretical fit obtained from least-squares analysis as described under Materials and methods. Integrated enthalpy change for each injection of compound into buffer is also shown (squares).

−10.5 kcal/M, this was offset by an unfavorable change in entropy, $T\Delta S$ of −4.10 kcal/M.

An ITC experiment with 2-phenyl-*N*-(5-piperazin-1-ylpentyl)quinazolin-4-amine (**4**) and 47/23mer DNA substrate produced a binding isotherm with nearly the same profile as the isotherm obtained for the pyridinyl quinolinediamine (data not shown). The data for compound (**4**) also fit two sets of independent binding sites model and indicated the affinity at one site was 1.6 µM while the other was again 10-fold less tightly bound at 15 µM. Thermodynamic parameters for the interactions were ΔH of −4.7 kcal/M, ΔG of −8.2 kcal/M and $T\Delta S$ of 3.5 kcal/M for the high affinity binding and ΔH of −15.8 kcal/M, ΔG of −6.8 kcal/M and $T\Delta S$ of −9.0 kcal/M for the low affinity binding.

As a control, binding of the known DNA intercalator, DAPI, was examined by ITC using the same experimental protocol as for the two previous compounds. A similar binding isotherm was obtained for DAPI as was obtained for compounds (**3**) and (**4**). The data for DAPI were slightly more scattered due to lower solubility of DAPI in the assay buffer but indicated about 200 nM affinity for the highest affinity site and 400 µM affinity for the lower affinity site. These affinities can only be judged as approximate since the model fit to the experimental data was not exact.

Protein crystallography

One of the primary reasons for biophysical investigations of various analogs of ATP or screening hits was to gain confidence that compounds were truly binding to the protein. This evaluation was a prelude to cocrystallization or crystal soaking experiments with lead compounds. Initial kinetic and binding data suggested that compound (**2**) was likely bound to HCV helicase. Therefore, a series of crystal soaking experiments were carried out with this and other putative inhibitors to determine if a complex with the compound could be prepared. Helicase protein crystals were soaked with compounds as indicated in the methods section. The crystal appeared to take up the compound and concentrate the highly colored compounds. Data were collected on these crystals and the structures solved by molecular replacement. However, a specific site of interaction for the compounds could not be found. These data would be consistent with multiple, nonspecific sites of interaction.

Discussion

Ligand perturbation of NS3 helicase denaturation and implications in the catalytic cycle

We have shown that some compounds were able to stabilize the hyperchromicity change of helicase under denaturing conditions (AMP-PNP), while other compounds including the substituted phenyl quinolinediamine and AMP-PCF_2P had the opposite effect. The ATP analogue data may provide insights into a mechanistic scheme for helicases [18]. However, because denaturation studies could not be carried out in the presence DNA substrate due to the increased thermal stability of the complex, mechanistic conclusions from these studies can only be suggestive. The HCV-binding data for AMP-PNP parallels that reported by Wigley et al. [18] for the bacterial helicase PcrA. Their crystallographic data suggest that ATP binding can induce large conformational changes in the multidomain helicase. The PcrA AMP-PNP bound conformation represents a very compact arrangement of domains 1 and 2, for example. Binding of AMP-PNP to HCV helicase may promote a similar domain rearrangement. One might expect that such a conformation would show greater resistance to denaturation in accordance with our observations (Fig. 5).

Furthermore, ADP bound to the protein should favor conformations that lead to translocation of DNA and eventual expulsion of ADP from the nucleotide-binding site. An ADP bound helicase may have increased flexibility or solvent exposure and hence an increased rate of denaturation in the ITD experiment. We have observed

such an increase at high ADP concentration (data not shown). Similar destabilization behavior was observed with the ATP analogue, AMP-PCF$_2$P (Fig. 4), suggesting that this analogue may be a better mimic of the ADP-bound conformation. However, we do not have detailed kinetic data to support this conclusion. In fact, a detailed kinetic evaluation of these ATP analogues has been difficult due to the greater than 200 μM K_d for ATP and low analogue solubility. Finally, the stabilization/destabilization of protein structure by nucleotide cofactors has been discussed for several decades. Structural and kinetic studies have clarified these states for some systems like the G-protein GTPases [19]. X-ray structures of HCV helicase with nucleotide analogues and/or DNA substrate will be needed in addition to kinetic studies to provide a similarly detailed view of the mechanism of HCV helicase.

Compound specificity

Several small molecule leads identified from HTS that were aimed at inhibiting hepatitis C virus NS3 helicase were evaluated to determine their affinity for helicase, binding specificity, and affinity for DNA substrate. Several of the leads were found to have low micromolar dissociation constants for NS3 helicase, including a phenyl substituted quinolinediamine (**2**) and the quinazolinamine (**4**). However, isothermal titration calorimetry experiments indicated a water soluble analog of compound (**2**), a pyridinyl substituted quinolinediamine salt (**3**), bound to the 47/23 mer DNA substrate with low micromolar affinity as did compound (**4**). Titration calorimetry data were consistent with both compound (**3**) and (**4**) intercalating into the DNA substrate. The phenyl-substituted quinolinediamine showed a lack of specificity for helicase since it also bound to flavodoxin in NMR experiments. Cocrystals with the compounds could not be prepared but the crystals acquired the color of the compound which suggested that the compounds occupied multiple nondiscrete binding sites on the protein surface. We conclude that none of the ligands tested had the necessary binding characteristics to proceed with further experimentation.

Acknowledgments

We thank Richard P. Swenson (The Ohio State University) for supplying the *D. vulgaris* flavodoxin, medicinal chemists at Pharmacia and Chiron for supplying the compounds to test, and Laura Tandeske (Chiron) for supplying the HCV NS3 helicase construct used in this work.

References

[1] D.E. Epps, R.W. Sarver, J.M. Rogers, J.T. Herberg, P.K. Tomich, The ligand affinity of proteins measured by isothermal denaturation kinetics, Anal. Biochem. 292 (2001) 40–50.
[2] N. Boyer, P. Marcellin, Pathogenesis, diagnosis and management of hepatitis C, J. Hepatology, Suppl. 32 (2000) 98–112.
[3] M.A. Walker, Hepatitis C virus: An overview of current approaches and progress, Drug Discovery Today 4 (11) (1999) 518–529.
[4] H.S Cho, N.C. Ha, L.W. Kang, M.C. Kyung, H.B. Sung, K.Y. Sung, B.H. Oh, Crystal Structure of RNA helicase from genotype 1b hepatitis C virus. A feasible mechanism of unwinding duplex RNA, J. Biol. Chem. 273 (1998) 15045–15052.
[5] J.L. Kim, K.A. Morgenstern, J.P. Griffith, M.D. Dwyer, J.A. Thomson, M.A. Murcko, C. Lin, P.R. Caron, Hepatitis C virus NS3 RNA helicase domain with a bound oligonucleotide: The crystal structure provides insights into the mode of unwinding, Structure 5 (1998) 89–100.
[6] N. Yao, T. Hesson, M. Cable, Z. Hong, A.D. Kwong, H.V. Le, P.C. Weber, Structure of the hepatitis C virus RNA helicase domain, Nature Struct. Biol. 4 (1997) 463–467.
[7] D.J.T. Porter, Inhibition of the hepatitis C virus helicase-associated ATPase activity by the combination of ADP, NaF, $MgCl_2$, and Poly(rU), J. Biol. Chem. 273 (1998) 7390–7396.
[8] M. Houghton, Q. Choo, J. Han, J. Choe, HCV NS3 protein fragments having helicase activity and improved solubility, Patent US6194140.
[9] C.E. Bystrom, D.W. Pettigrew, S.J. Remington, B.P. Branchaud, ATP Analogs with non-transferable groups in the γ position as inhibitors of glycerol kinase, Bioorg. Med. Chem. Lett. 20 (7) (1997) 2613–2616.
[10] V.V. Plotnikov, J.M. Brandts, L. Lin, J.F. Brandts, A new ultrasensitive scanning calorimeter, Anal. Biochem. 250 (1997) 237–244.
[11] E.R. Malinowski, D.G. Howery, Factor Analysis in Chemistry, Robert Krieger, Malabar, FL, 1989.
[12] R.W. Sarver, W.C. Krueger, An infrared and circular dichroism combined approach to the analysis of protein secondary structure, Anal. Biochem. 199 (1991) 61–67.
[13] J.P. Hennessey Jr., W.C. Johnson Jr., Information content in the circular dichroism of proteins, Biochemistry 20 (1981) 1085–1094.
[14] L.A. Compton, C.W. Johnson Jr., Analysis of protein circular dichroism spectra for secondary structure using a simple matrix multiplication, Anal. Biochem. 155 (1986) 155–167.
[15] P.J. Hajduk, E.T. Olejniczak, S.W. Fesik, One-dimensional relaxation- and diffusion-edited NMR methods for screening compounds that bind to macromolecules, J. Am. Chem. Soc. 119 (1997) 12257–12261.
[16] L. Lin, A.B. Mason, R.C. Woodworth, J.F. Brandts, Calorimetric studies of the binding of ferric ions to ovotransferrin and interactions between binding sites, Biochemistry 30 (1991) 11660–11669.
[17] G.L. Bryant, Jr., M.S. Harris, E.T. Baldwin, L. Tandeske, K.R. Shoemaker, B.C. Finzel, HCV Helicase RNA-binding domain flexibility quantified by comparison of multiple crystal forms, American Crystallographic Association Meeting, Buffalo, NY, May 22–27, 1999.
[18] S.S. Velankar, P. Soultanas, M.S. Dillingham, H.S. Subramanya, D.B. Wigley, Crystal structures of complexes of PcrA DNA helicase with a DNA substrate indicate an inchworm mechanism, Cell 97 (1999) 75–84.
[19] S.R. Sprang, G Protein mechanisms: Insights from structural analysis, Annu. Rev. Biochem. 66 (1997) 639–678.